Conf-9405191--1

LA-UR- 94-1613

Title: IRON OXIDE MINERAL-WATER INTERFACE REACTIONS STUDIED BY AFM

Author(s): M. E. Hawley
P. S. Rogers

Submitted to: Scanning Microscopy
Toronto, Canada
May 7-19, 1994

MASTER

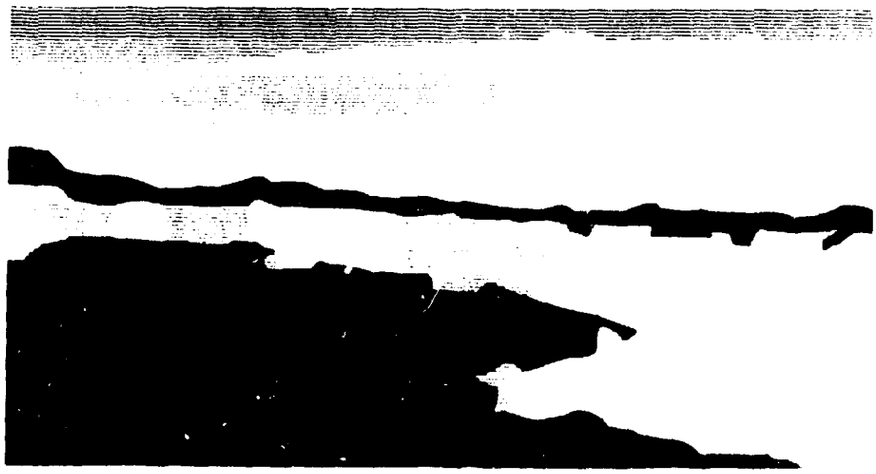

Los Alamos
NATIONAL LABORATORY

Title: Iron Oxide Mineral-Water Interface Reactions Studied by AFM

Authors: M. E. Hawley and P. S. Z. Rogers

Location: Scanning Microscopy International 1994 meeting, Toronto, Canada, 7-12 May 1994.

Abstract:

Natural iron mineral surfaces have been examined in air by atomic force (AFM) and scanning tunneling (STM) microscopies. A number of different surface features were found to be characteristic of the native surface. Even surfaces freshly exposed by crushing larger crystals were found to have a pebbly surface texture caused by the presence of thin coatings of what might be surface precipitates. This finding is interpreted as evidence for previous exposure to water, probably through an extensive network of microfractures.

Surface reactions on the goethite crystals were studied by AFM at size resolutions ranging from microns to atomic resolution before, during, and after reaction with distilled water and 0.1N HCl. Immediate and extensive surface reconfiguration occurred on contact with water. In one case, after equilibration with water for 3 days, surface reprecipitation, etching and pitting were observed. Atomic resolution images taken under water were found to be disordered. The result of surface reaction was generally to increase the surface area substantially through the extension of surface platelet arrays, present prior to reaction.

Draft 1 date 4/29/94

Introduction:

Iron oxide natural minerals are important in ground-water/mineral sorption, dissolution, and reaction processes. In addition to their presence in bulk form, they are frequently present on the surface of other minerals both on the outer surface and in cracks and fissures in the rock. Surface reactivity of these materials is influenced by a number of factors: composition, crystallographic face, the presence of surface precipitates, and the number of reactive sites. In turn, the number of reactive sites is a measure of the surface morphology, e.g. screw dislocations, planar steps and kink sites (surface roughness), and density of chemical defects, e.g. substitutions or vacancies. Very little work has been done on the characterization of iron oxide mineral surfaces in their native state. Without a knowledge of the actual surface structure as well as the chemical make-up of the mineral surfaces under investigation, bulk sorption measurements can not shed light on the actual mechanism of mineral-water interface processes and, therefore, can not explain the differences that exist between results obtained from bulk sorption measurements on natural versus synthetic mineral samples. Compositional deviation from that of the host mineral can be localized at the surface and concentrated laterally in small regions. Atomic compositional variations due to doping at Fe sites, which is very common, is not necessarily uniform across a surface. Some of these inhomogeneities result from weathering processes of unknown history; the minerals have already been exposed to gases and/or liquids of unknown composition. Discrepancy between bulk sorption measurements on natural and synthetic mineral samples could then be argued on the basis of the presence or absence of surface alteration or surface coatings resulting from weathering conditions. Unlike experiments carried out on synthetic minerals, an exact

This work was supported by the Yucca Mountain Site Characterization Project Office as part of the Civilian Radioactive Waste Management Program. This project is managed by the US Department of Energy, Yucca Site Characterization Project. The Yucca Mountain Project Technical Data Catalog Tracking Number is (to be filled in later)

knowledge of the immediate surface composition is not known for natural minerals.

Although a number of techniques are available to characterize mineral surfaces, few if any can meet both the stringent depth and lateral resolution constraints necessary to identify local chemical and structural variations, making these techniques of limited value for near surface characterization. The scanning tunneling (STM) and atomic force (AFM) microscopes, although unable to provide surface analytical information, are increasingly being used to provide local nano- and atomic resolution mineral surface structural information not previously available by other methods [Hartman et. al., 1990; Hochella, 1990; Hochella et. al. 1989,1990; Eggleston and Hochella, 1990a, 1990b, 1991, 1992, 1993; Manne, et. al., 1990, 1991; Johnsson et. al., 1991; Hillner, 1992b; Drake, 1991; Gratz, 1991; and Rachlin et. al., 1992]. This capability is particularly important for the study of natural mineral surfaces. The added advantage of being able to image these surfaces under solution has allowed a number of researcher to successfully exploit these techniques for in situ studies of mineral-water reactions and sorption processes [Eggleston and Hochella, 1991,1993; Manne, et. al., 1991; Hansma, et. al., 1991a, 1991b; Weisenhorn, et. al., 1990; Weisenhorn, et. al., 1991; and Prater, et. al., 1991]. Studies carried out on calcite [Hillner, et. al., 1992a, 1992b] and hematite [Eggleston, et. al., 1993] have shed new light on dissolution and growth mechanisms and ion adsorption at the atomic level, respectively.

The present study focused on a family of iron oxide minerals which includes hematite, goethite, magnetite, and maghemite. Goethite is often found as a weathering product of magnetite and often associated with hematite [Roberts, et. al., 1990]. Hematite, which is a semiconductor, always possesses oxygen vacancies and donor defects [Shuey, 1975], and is dimorphous with maghemite. At saturation of oxygen vacancies magnetite is formed. The iron in goethite, hematite, and maghemite is in the Fe^{+3} oxidation state, while in magnetite the iron is mixed Fe^{+2} and Fe^{+3} [Roberts, et. al., 1990].

Problems related to understanding the reactivity of natural mineral surfaces can't be completely resolved by studying the same reactions using their synthetic counterparts. Disparities in reactive response, even from one sample

to another, are expected due to differences in surface sorbates, surface roughnesses, and compositional variations. As a consequence, the approach taken here in this study was three fold: first, to examine a number of natural mineral crystals to identify characteristic native goethite surfaces and second, to cleave crystals to obtain surfaces suitable for atomic imaging, and third, to study, in situ, mineral-water interface reactions on selected characterized surfaces. The nature of surface roughening due to reaction with the water was deemed important for identification of the reactive sites expected to participate in sorption processes. Differences in reactive response of various surfaces are expected to give clues to the presence of surface precipitates and defects and to differences in reactivity of crystal sites.

Experimental:

Characterization:

All imaging was carried out on a Nanoscope III STM and AFM [Digital Instruments, Inc., Santa Barbara, CA]. Pr/Ir, both cut and etched, tips were used for STM imaging. All AFM data was obtained using commercial Si_3N_4 oxide-sharpened tips attached to 100 μm long triangular cantilevers. For STM imaging, electrical contacts were made with Ag conductive paint.

Natural blades α-goethite (α-FeO(OH)), Brazilian α-hematite (α-Fe_2O_3), and Yucca Mountain magnetite, Fe_3O_4, were examined in these experiments. Since goethite is insulating, the surface micro- and nano-structure of about fifteen natural environmentally weathered α-goethite crystals and crystal fragments were extensively characterized using the AFM. The platy orthorhombic α-goethite crystals used in this study were shiny blackish brown but appeared orangish brown when crushed. The published α-goethite lattice constants are: a = 4.596, b = 9.957, and c = 3.021 [Roberts et. al.]. Goethite is expected to cleave unevenly, along {010} perfectly and {100} distinctly. Samples 1-9 were examined as received, while 10 through 15 were fragments obtained by crushing a larger crystal by fracturing it between glass slides in an attempt to obtain freshly cleaved surfaces suitable for atomic imaging. This

procedure was followed because the crystals were small and brittle, tending to crumble rather than break cleanly along crystallographic planes.

About nine hematite crystal fragments were also examined. The trigonal Brazilian α-hematite crystals were metallic to semiconductive and lustrous black in color. The expected lattice parameters are: a = 5.0317 and b = 13.737 The hematite samples were chipped from a large tabular crystal, arranged in a rosette referred to as an "iron rose" [Roberts, et. al., 1990], using a hammer and chisel. No perfect cleavage is expected for hematite but parting is predicted along twinning directions {0001} and {10$\bar{1}$1}. Frequently inclusions of mica and possibly quartz were observed on the freshly cleaved surfaces. The semiconductive behavior of this sample was indicative of substantial doping, possibly with Ti or Mg [Shuey, 1975].

The surface of five magnetite crystals were imaged. The magnetite samples were mechanically extracted from Yucca Mountain tuff and were quite small, usually < 50 to 100 μm in breadth and dull gray to black. Because of the small sample sizes, a 5 mil nicrome wire was use to position the crystals onto the double sided adhesive tape or Ag colloid paint used to hold the sample in position while imaging. Magnetite is cubic with a lattice constant a = 8.374.

Reactions:

Two of the original nine goethite crystals examined were used in reaction experiments. After characterization of their surfaces, the first experiment was carried out in two stages on crystal #8, the first reaction under high resistance ultra pure water (pH = 5.5 to 7.5 at 25 C) and the second one under 0.1 N HCl. In both cases, fluid was introduced into the AFM wet cell via a syringe pump at a slow continuous uncalibrated rate, thus continuously exposing the mineral surface to fresh pure solution. Crystal #9, which exhibited a number of interesting surface features, primarily on nearly atomically smooth surfaces, was only reacted with pure water.

Results:

Characterization:

The topographical images of the crystal surfaces used in this experiment revealed a number of different but characteristic features, appearing repeatedly from one sample to another. The complexity of the problem of interpreting the images to unravel the surface structure and composition was immediately apparent. Many of the surfaces were covered with faceted crystallites, ranging in size from 100's of nm to a couple of μm's. Other surfaces appeared to be covered by an amorphous layer of unknown material. The apparent coating often consisted of shapeless mounds. Striations suggestive of planar edges were frequently observed on the goethite crystal surfaces, fig. 1a. This finding is not surprising considering the imperfect cleavage of many of these iron oxide crystals. These surfaces would present a large number of reactive sites. For that reason one would be expected them to be either already altered from the bulk or vigorously responsive to a reactive environment.

Atomically smooth surfaces with step edges a few angstrom's high were often observed; the surfaces usually displayed a pebbly texture, sometimes possessing low level ordering, but rarely clear crystallographic structure, fig. 1b. Step heights obtained from line scans across images often matched dimensions in the unit cell. In one case a screw dislocation was observed.

The surface of crystal #9 was largely atomically smooth, with sufficient crystal features, i. e. cleavage angles and atomic steps, to support assignment to the goethite (010) face, the preferred cleavage plane, fig. 2a and b. Additionally, atomic resolution images were obtained on this surface, fig. 3a. Scattered regions covered by ordered arrays of ~ 5 Å high platelets a few μm's long were found. The arrays consisted of rows of platelets, about 200 to 300 $Å^2$ which terminated at one end into uniform triangles, fig. 4a. The extent of any one array rarely exceeded a few μm's. Although no compositional data could be obtained by AFM, the heights of these platelets were approximately one half the (010) unit cell **b** parameter. The crystal structure of goethite possesses parallel channels every 5 Å, where fracturing of the unit cell is expected to take place, see figure 5 (Parfitt, et. al. 1976).

The surfaces of the hematite crystals also exhibited a wide variety of microstructures, many of which could have been due to surface precipitates. In general, the micro- to nano-surface structures displayed a high degree of ordering, even though atomic imaging was rarely achieved, fig. 6a and b. High quality atomic STM images were obtained on a few crystal fragments, and were found to be bias dependent. Two images, taken sequentially at the same tunneling current but in different tunneling directions, are shown in fig. 7a & b. Both show a periodic array of atomic features with the same interatomic spacing. Under careful examination one can see that the rows of bumps and holes reverse on bias reversal from one image to the other; these results are consistent with the notion that one can selectively sample either the filled, negative sample bias, or empty electronic states, positive sample bias, by changing the tunneling direction. The invariance of the atomic spacing (Å) suggests that a simple interpretation that oxygen atoms are imaged during negative sample bias while Fe atoms are imaged when the sample bias is positive is probably a simplified picture of the electronic states being sampled.

Another atomic resolution image from the hematite crystal surface contains bands of alternating lighter and darker contrast, fig. 8. One might first assume that the tunneling tip has picked up contamination, lowering the tunneling current, and then discarded it while scanning across the surface. On closer examination, however, one can clearly identify kink sites in rows of atoms where the switch-over in contrast takes place. An alternate interpretation is that the surface atoms with lower contrast are the sites of attached ions, e. g., hydroxyl groups, or water molecules.

Because the magnetite samples were optically rough and dull gray, atomic resolution images were not expected. However, images of locally atomically smooth planar regions were found, but these were covered with nano-size particulates. When the AFM tip was positioned only a few 10 of µm's away from the smooth area, the surface was found to be quite different, covered either by an amorphous billowy looking material or by a field of pyramidal faceted peaks.

Reactions:

Two distinct water reactions occurred with the two different goethite crystals. Optically, the pre-water surface of the first crystal, #8, contained a number of large pits which did not appear in the AFM images, suggesting that the surface was coated with a transparent precipitate. This amorphous coating, fig. 9a, reacted immediately on contact with water, releasing a gaseous substance. The gas had to be expelled from the wet cell and the split diode detector realigned before proceeding with imaging. The pits and fissures, missing from the pre-reaction AFM images, suddenly appeared after water exposure, fig. 9b. Because the water was slightly acidic, CO_2 is a likely candidate for the reactant gas, suggesting calcite as a possible coating. After a 24 hour water exposure, the surface structure became web-like and soft. Many of the images taken under water were smeared and appeared blurry.

Exposure of the crystal #8 surface, this time to a 0.1 N HCl solution, resulted in further development of the web-like features. Although the appearance of holes and crevices on the surface added to the root-mean-square (RMS) roughness, initially the RMS value decreased; the decrease was primarily due to a reduction in the size of the amorphous hillocks. Later, however, as a function of reaction time and acid exposure, the overall surface area increased as the web-like network of small holes or pits evolved (fig. 9c). No atomic resolution images were obtained from these newly "cleaned" surfaces.

Reaction of crystal #9 with water exhibited both dissolution and reprecipitation. The water-mineral interface reaction was faster than the few seconds set-up time for filling the AFM wet cell with water, then realigning the optical detection time. To the AFM the reaction appeared immediate. On reaction with continuously replenished fresh water, the arrays of platelets on the (010) crystal face grew significantly in lateral extent, fig 10a, b, and c. Significant sharpening of the platelet matrix was noted as the reaction progressed (fig. 11). The line formed by the termination of the rows of platelets transformed into a scalloped edge with 90° angles separating segments, fig 4b. After exposure to stagnant water for three days, both pitting, fig. 12a and b, and reprecipitation along crystal directions, fig. 13a and b were observed. Note that as the reaction

progressed, the surface participated as much as step edges, where the reaction rate was expected to be significantly faster.

Atomic resolution images were obtained under water within a flat rectangular area at the perimeter of an array, fig. 3b; a corner of this region is visible in the lower right corner of fig. 11. Although the structure is disordered, the amplitude of the atomic features is 10 times that in the pre-reaction image. These features were reproducible, scaling correctly with the scan range. Since the reaction was still proceeding, the lack of clean crystallographic is not surprising. The amplitude of post reaction atomic features returned approximately to pre-reaction values. A second area, smooth enough for atomic imaging, but which could not be resolved to the atomic scale, possessed a high degree of ordering of 50 Å features, fig. 14.

One localized area, which prior to reaction was covered with crystallites, fig. 15a, was re-imaged after reaction, fig. 15b. The dissolution of the crystallites appeared to have been slow; they had not completely disappeared after the 3-day period sitting under water. The size of the crystallites was significantly reduced, with a concomitant decrease in surface roughness.

Conclusions:

All of the native crystals whose surfaces were imaged in this study displayed a wide variety of structural features; many of these different structures appeared on several different crystals. We believe that some of these structures belong to surface precipitates while others are due to weathering of the surface. Most of the smooth surfaces imaged possessed a pebbly texture that could not be atomically resolved to obtain crystallographic information. Step edges tended to be rounded with cleavage plane intersections curved rather than sharp angular breaks. This finding is consistent with the conclusion that the surfaces have previously been exposed to weathering conditions, and that the crystals tend to cleave along already existing cracks where there has been ground water contact. Indeed most surfaces, even those created by fracturing crystals, appeared to be coated or eroded. This finding could have serious implications for interpretation of bulk sorption measurements, because it indicates that the bulk composition and chemistry of the mineral does not necessary control

surface adsorption properties. If essentially all of the reactive surface area has already undergone prior reaction with ground water, the surface chemistry could be modified by whatever substance is precipitated or adsorbed onto the surface. The history of the sample then would be more important than its bulk chemistry in determining future adsorption behavior. We have observed this precise effect in the natural crystals.

Water and acid-mineral interface reactions were carried out on an unidentified crystal face; initially, a gaseous material was liberated. Further reaction resulted in creation of a web-like surface, possible evidence for the (001) surface which has channels perpendicular to the surface.

We have successfully obtained atomic resolution images of the (010) crystal face of crystal #9 α-goethite. The poor quality of the images taken in air is attributable to adsorbates on the surface. Images of the atomic structure taken under water were highly disorder due to the reaction processes. Cleavage angles, step heights, and the ordered array of surface platelets support this identification. In the latter case, the increase in the size of these platelet arrays, along with their 5 Å height, suggests that the platelets consist of goethite which is undergoing dissolution during reaction with water. Extensive pitting and peeling of the crystal took place a approximately the same rate as reaction at the edges of platelet arrays. This suggests that this is a highly reactive surface. On sitting in stagnant water, material was reprecipitated onto the surface along crystallographic directions. Although surface microcrystallites present on crystal #8 reacted quickly while those on crystal #9 dissolved very slowly, we conclude that neither coating is goethite.

Bibliography

Drake, B., Prater, C. B., Weisenhorn, A. L., Gould, S. A. C., Albrecht, T. R., Quate, C. F., Cannell, D. S., Hansma, H. G., and Hansma, P. K., (1989), "Imaging Crystals, Polymers, and Processes in Water with the Atomic-Force Microscope", *Science* **243**, pp. 1586.

Eggleston, C. M. and Hochella, Jr., M. F., (1990), "Scanning Tunneling Microscopy of Sulfide Surfaces", *Geochim. Cosmochim. Acta* **54**, pp. 1511–1517.

Eggleston, C. M. and Hochella, Jr., M. F., (1991), "Scanning Tunneling Microscopy of Galena (100) Surface Oxidation and Sorption of Aqueous Gold", *Science* **254**, pp. 983-986.

Eggleston, C. M. and Hochella, Jr., M. F., (1992), "The Structure of Hematite {001} Surfaces by Scanning Tunneling Microscopy: Image Interpretation, Surface Relaxation, and Step Structure", *American Mineralogist* **77**, pp. 911-922.

Eggleston, C. M. and Hochella, Jr., M. F., (1993), "Tunneling Spectroscopy Applied to PbS(001) Surfaces: Fresh Surfaces, Oxidation, and Sorption of Aqueous Au", *American Mineralogist* **78**, pp. 877-883.

Gratz, A. J., Manne, S., and Hansma, P. K., (1991), "Atomic Force Microscopy of Atomic-Scale Ledges and Etch Pits Formed During Dissolution of Quartz", *Science* **251**, pp.1343-1346.

Hartman, H., Sposito, G., Yang, A., Manne, S., Gould, S. A. C., and Hansma, P. K., (1990), "Molecular-Scale Imaging of Clay Mineral Surfaces with the Atomic Force Microscope", *Clays and Clay Minerals* **38**, pp. 337-342.

Hillner, P. E. Gratz,, A. J., and Hansma, P. K., (1992a), "Composite Spiral Growth Kinetics of Calcite Revealed by AFM", Proceedings of the International Society for Optical Engineering, *SPIE 1639 Scanning Probe Microscopies*,, pp. 160-170.

Hillner, P. E. Gratz,, A. J., Manne, S., and Hansma, P. K., (1992b), "Atomic-Scale Imaging of Calcite Growth and Dissolution in Real Time",*Geology* **20**, pp. 359-362.

Hochella, Jr., M. F., (1990), "Atomic Structure, Microtopography, Composition, and Reactivity of Mineral surfaces", in *Mineral-Water Interface Geochemistry*, eds. M.F. Hochella, Jr. and A. R. White, Reviews in Mineralogy **23**, pp. 87-132.

Hochella, Jr., M. F., Eggleston, C. M., Elings, V. B., Parks, G. A., Brown, Jr., G. E., Wu, C. M., and Kjoller, K., (1989), "Mineralogy in Two Dimensions: Scanning Tunneling Microscopy of Semiconducting Minerals with Implications for Geochemical Reactivity", *American Mineralogist* **74**, pp. 1233-1246.

Hochella, Jr., M. F., Eggleston, C. M., Elings, V. B., and Thompson, M. S., (1990), "Atomic Structure and Morphology of the Albite {010} Surface:An Atomic-Force Microscope and Electron Diffraction Study", *American Mineralogist* **75**, pp. 723-730.

Johnsson, P. A., Eggleston, C. M. and Hochella, Jr., M. F., (1991), "Imaging Molecular-Scale Structure and Microtopography of Hematite with the Atomic Force Microscope", *American Mineralogist* **76**, pp. 1442-1445.

Manne, S., Butt, H. J., Gould, S. A. C., and Hansma, P. K., (1990) "Imaging Metal Atoms in Air and Water Using the Atomic Force Microscope", *Appl. Phys. Lett.* **56** (18), pp. 1758-1759.

Manne, S., Hansma, P. K., Massie, J., Elings, V. B., Gewirth, A. A., (1991), "Atomic-Resolution Electrochemistry with the Atomic Force Microscope: Copper Deposition on Gold", *Science* **251**, pp. 183-186.

Parfitt, R. L., Russell, J. D., and Farmer, V. D., (1976), "Confirmation of the Surface Structures of Goethite (α-FeOOH) and Phosphated Goethite by Infrared Spectroscopy", *J. C. S. Faraday I* **72**, pp. 1082-1087.

Prater, C. B., Wilson, M. R., and Garnaes, J., (Mar/Apr 1991), "Atomic Force Microscopy of Biological Samples at Low Temperature", *J. Vac. Sci. Technol.* **B 9** (2), pp. 989-991.

Rachlin, A. L., Henderson, G. S., and Goh, M. C., (1992), "An Atomic Force Microscope (AFM) Study of the Calcite Cleavage Plane: Image Averaging in Fourier Space", *American Mineralogist* **77**, pp. 904-910.

W.L. Roberts, T.J. Campbell, and G.R Rapp, Jr., *Encyclopedia of Minerals*, second edition, (Van Nostrand Reinhold, NY, NY, 1990) pg. 356-357.

Shuey, R. T., (1975), "Hematite - α-Fe_2O_3", Semiconducting Ore Minerals (Elsevier Scientific Publishing Company, N.Y., N. Y., 1975), Chapter 21 pp. 358-370.

Weisenhorn, A. L., Egger, M., Ohnesorge, F., Gould, S. A. C., Heyn, S. -P., Hansma, H. G., Sinsheimer, R. L., Gaub, H. E., and Hansma, P. K., (1991), "Molecular-Resolution Images of Langmuir-Blodgett Films and DNA by Atomic Force Microscopy", *Langmuir* **7** (1), pp. 8-12.

Weisenhorn, A. L., MacDougall, J. E., Gould, S. A. C., Cox, S. D., Wise, W. S., Massie, J., Maivlad, P., Elings, V. B., Stucky, G. D., and Hansma, P. K., (1990), "Imaging and Manipulating Molecules on a Zeolite Surface with an Atomic Force Microscope", Science **247**, pp. 1330-1333.

Figure captions:

Figure 1: Two AFM images taken from the same goethite crystals showing typical native mineral surfaces. (a) The left-hand surface, RMS = 26 Å, consists of parallel striations about 50 nm wide and 2 - 5 nm high. (b) Surface steps, 10 - 30 Å high, are visible in the second image. The pebbly surface texture has ~ 20 nm granularity, with a RMS roughness measured at 10 Å. The lateral scale in both images is µm's.

Figure 2: Images were taken from an atomically smooth region on goethite crystal #9. Image (a) is a 5 μm^2 scan area with 152° cleavage angle visible. The large surface step is about 150 Å high. The parallel horizontal strips are not artifacts but one unit cell high steps on the (010) crystal face. ~ 10 Å. Note that the array, bottom right and that, upper left, align with the large surface step. (b) A close up of the surface steps and part of a platelet array whose rows of extend over the step edges. The scan is 1.7 μm^2. The angle formed by the upper termination of the rows is approximately 150°.

Figure 3: 8 nm^2 AFM atomic resolution images from goethite crystal #9 native surface taken before reaction with water, (a), and under water, (b), as the reaction was proceeding. Contaminates on (a) limited the images quality and crystallographic information. Image (b) was distorted by the reaction process but was reproducible.

Figure 4: These AFM images, also taken on the surface of crystal #9, show an array of surface platelets, 20 - 30 nm across and ~ 4 - 5 Å high, as they appeared before reaction (a) and after reaction (b). Note that the triangular arrangement of platelets at the termination end of the array in (a) become scalloped, (b). In the latter case, the edge segments are rotated from each other by 90°. Both images are about 730 nm^2.

Figure 5: a-Goethite atomic structure, shown in two projections (modified from Parfitt, et. al. 1975). Note the open channel parallel to the [100] direction located at (5 Å) which is one-half **b** (10 Å), the [010] direction. The goethite crystal is expected to cleave along this channel, every 5 Å..

Figure 6: 868 nm^2 STM topographs taken of two typical natural surfaces found on the Brazilian α- hematite samples. The STM cannot determine if these surface structures are due to precipitates, reaction products, or hematite. The background granularity, as well as the elongated array of fingers growing out from the surface, in image (a) are highly ordered with a RMS roughness ~ 90 Å. The highly ordered textured surface in (b) consists of 80 Å nano-grains (RMS = 9 Å).

Figure 7: Sequential atomic resolution images taken with the STM on a freshly cleaved hematite surface. Image (a) was taken with a sample bias = + 1.1 eV while image (b) was taken with the sample bias reverse, - 1.1 eV .

The set point current in both cases was 0.3 nA. Note that the atomic spacing does not change but that the "holes" in (a) become "bumps" (b).

Figure 8: STM atomic resolution image taken on the same sample as in fig. 6. Features with lower vertical contrast, although possibly due to tip contamination, follow atomic rows and kink sites rather that straight lines along the tip scan

Figure 9: Three 6.7 μm^2 AFM images taken on the surface if goethite crystal #8. Image (a), RMS = 114 Å, upper left, was taken in air prior to reaction of the surface with water or 0.1 N HCl. Image (b), upper right, RMS = 457 Å, was taken under water. Note the holes and crack which were optically visible but did not appear in the AFM images until the surface was reacted with the water. The surface of the goethite in image (c), lower left, taken under a solution of 0.1 N HCl, has developed a web-like structure possibly due to removal of inclusion or the presence of channels in the goethite crystal structure.

Figure 10: Three 2 μm^2 AFM images taken on goethite crystal #9 surface, (a), upper left, before water reaction (RMS = 5.5 Å), (b), upper right, during under flowing water (RMS = 8.7 Å), and (c), lower left, dried after 3 days reaction in stagnant water (RMS = 7.1 Å). Although all three surfaces are relatively smooth, they differ significantly in structure. The ordered array of platelets is seen to grow significantly in extent as the reaction progressed. Since fresh water was continuously introduced to the sample surface during the initial reaction stage, dissolution rather than reprecipitation is probably responsible.

Figure 11: This AFM micrograph of the dry goethite surface at higher resolution, 500 nm^2, shows sharpening of the platelet array matrix edges after the reaction.

Figure 12: Extensive scaling (a), RMS = 14 Å, and pitting (b), RMS = 17 Å, of the surface are clearly shown in these 3 μm^2 AFM micrographs. The on unit cell high triangular scaling in the lower right-hand corner of image (a) only appeared as the reaction progressed. The large pit in the upper left of image (b), one cell nigh, has an array transversing it. Note the extensive pitting on this surface, reminiscent of image fig. 9 c.

Figure 13: Two 2 μm^2 AFM images taken on a second area of goethite crystal #9 surface, before (a), RMS = 35 Å, and after (b), RMS = 67Å, water reaction. This surface had been exposed to stagnant water for three days during which reprecipitation along crystallographic direction has occurred with an increase in surface roughness.

Figure 14: Smooth post-reaction highly ordered surface with 40 - 50 Å features, RMS = 1.6 Å. Despite the surface ordering attempts at atomic imaging were unsuccessful.

Figure 15: 1.8 μm^2 AFM images (a), RMS = 117 Å, and (b), RMS = 76 Å, were taken on a third area of crystal #9 prior to reaction with water and after the reaction was completed, respectively. The surface was covered with microcrystallites which appeared to slowly dissolve at a slower rate the clean surface reacted.

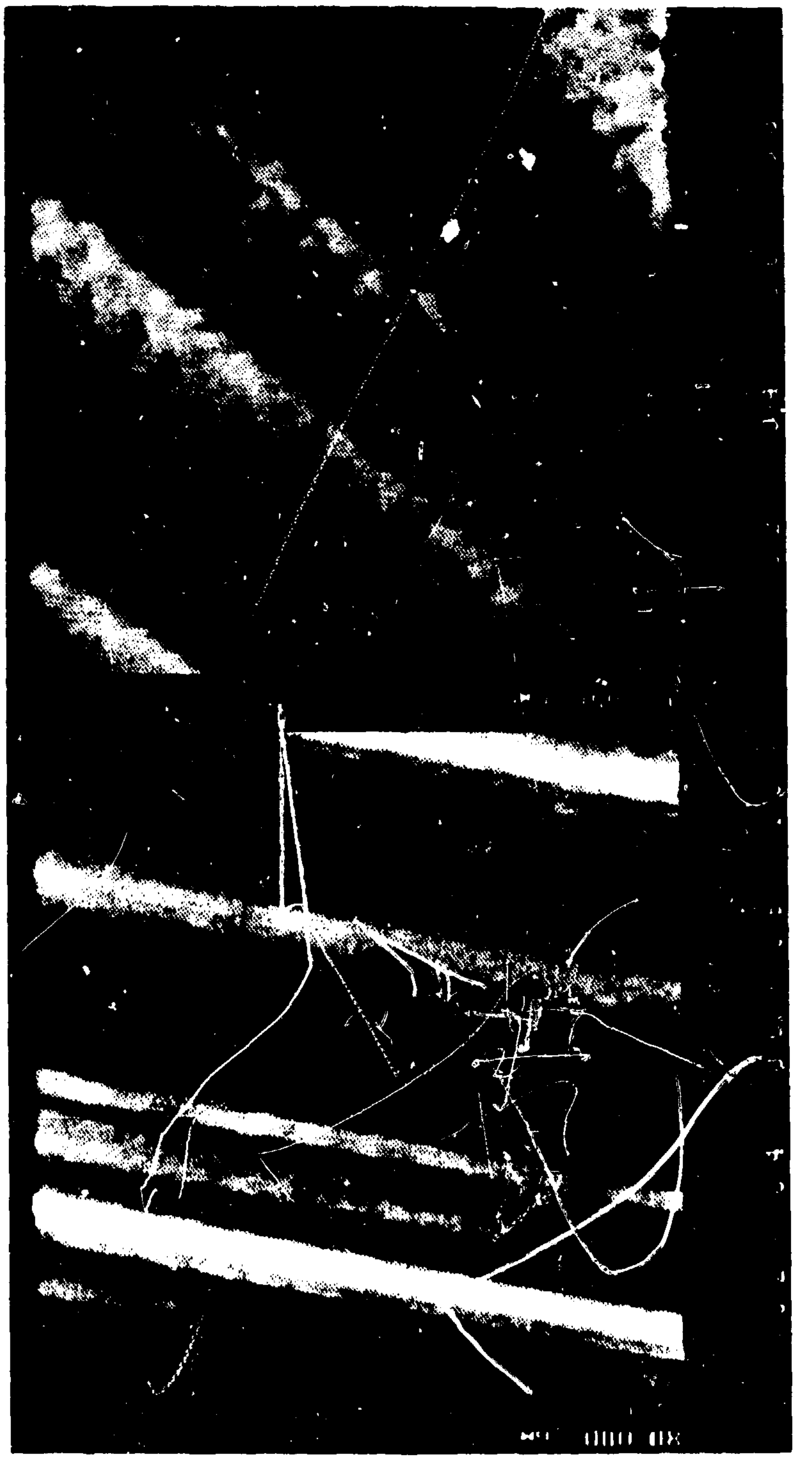

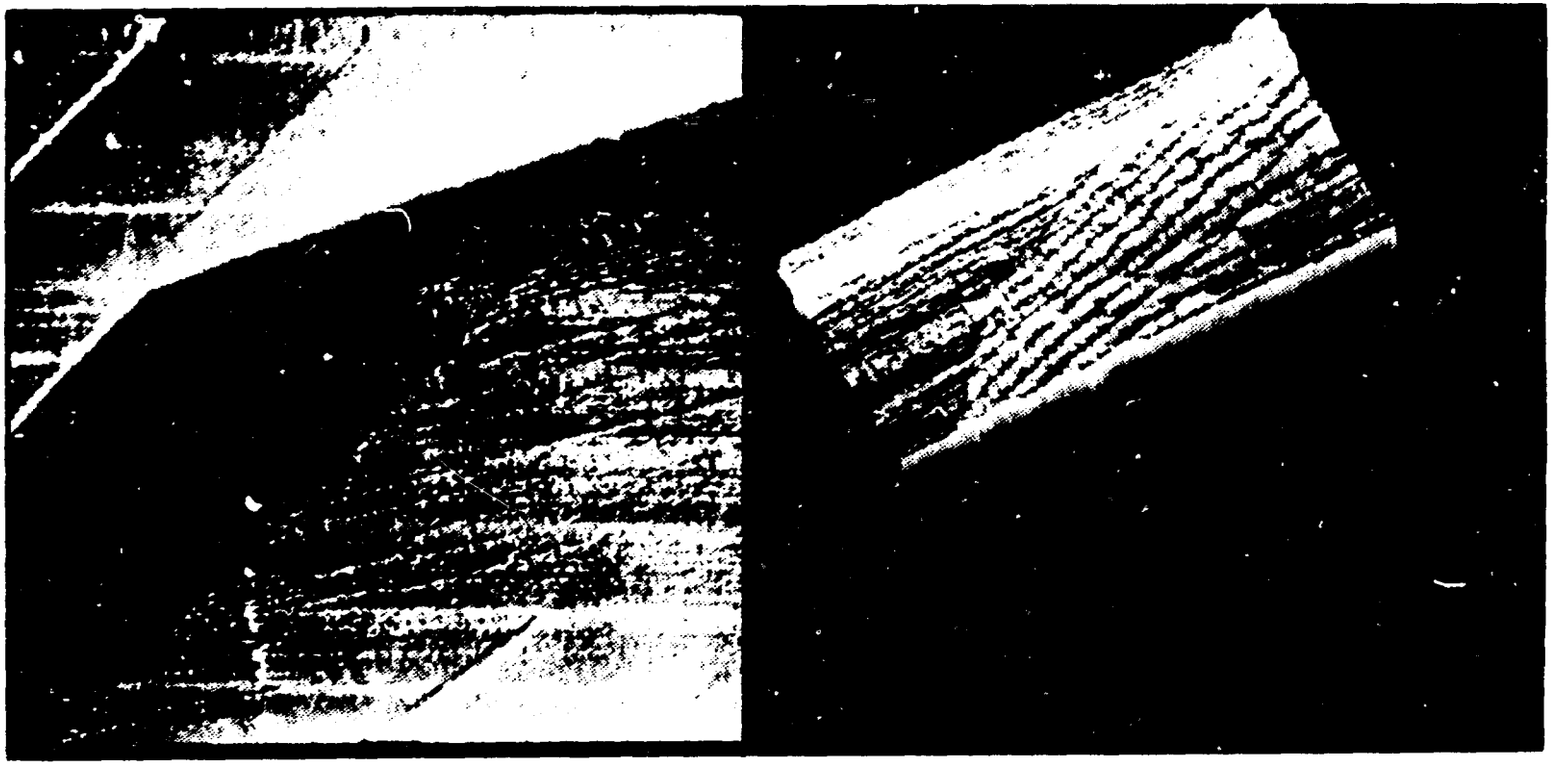

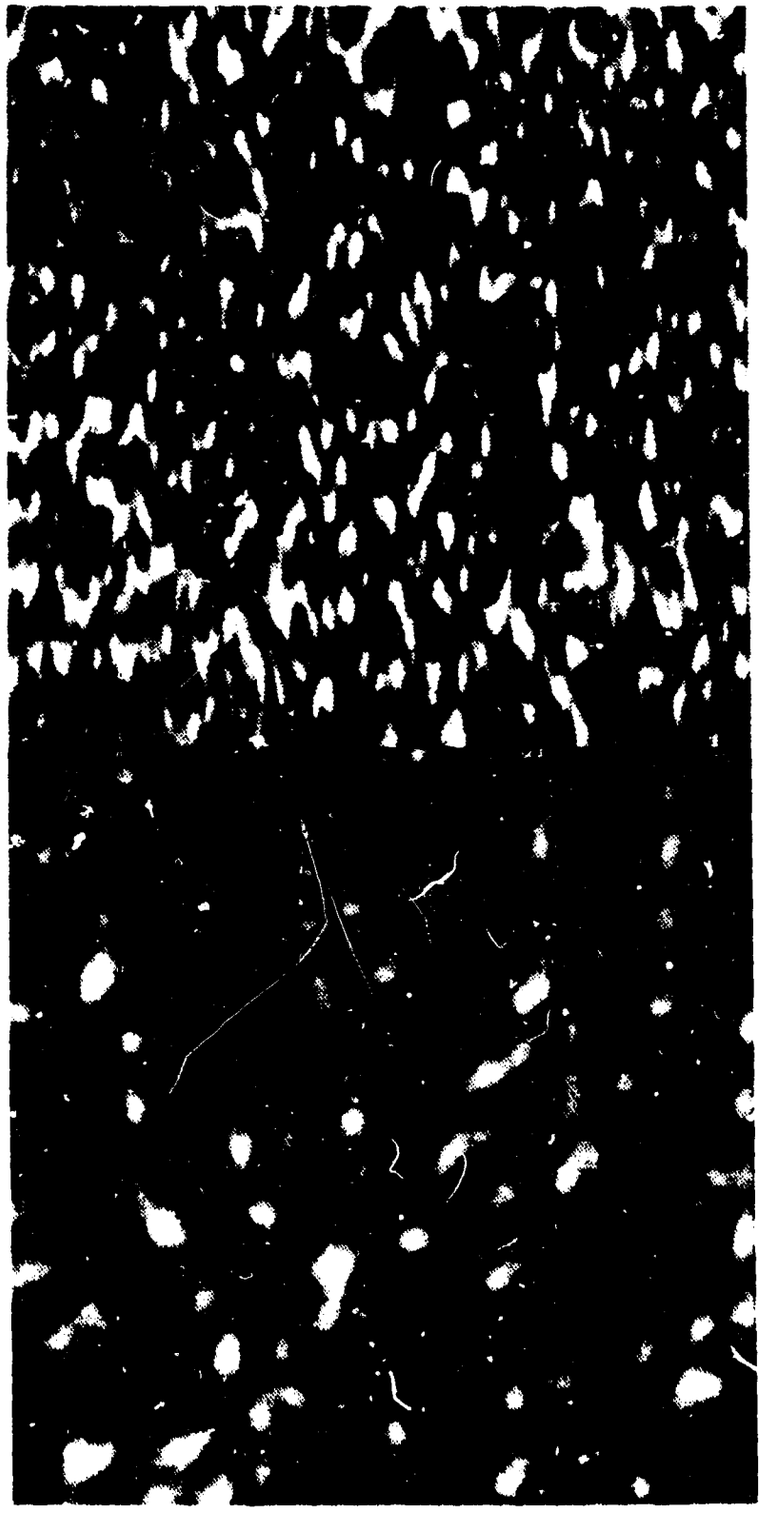

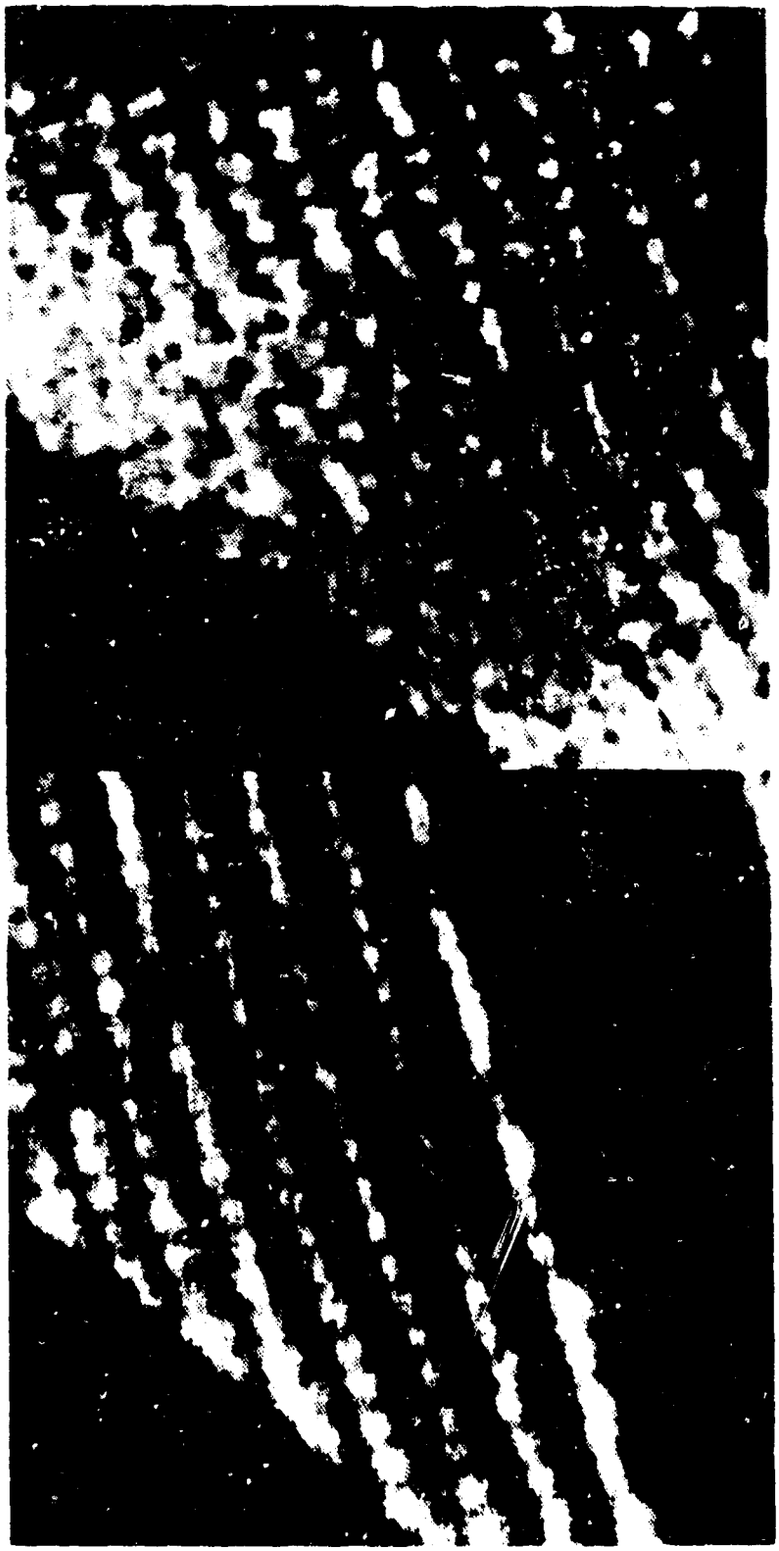

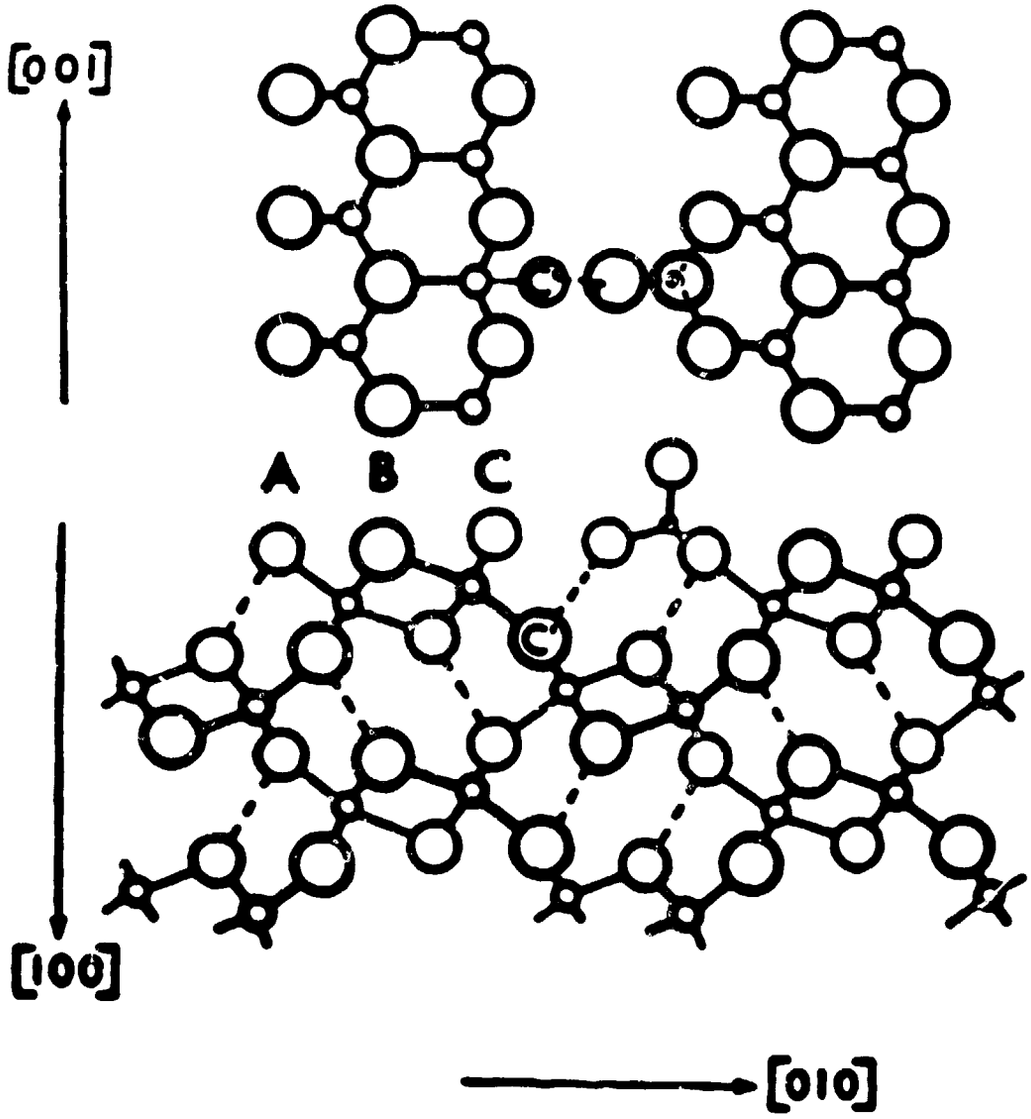
[001]
A
B
C
[100]
[010]

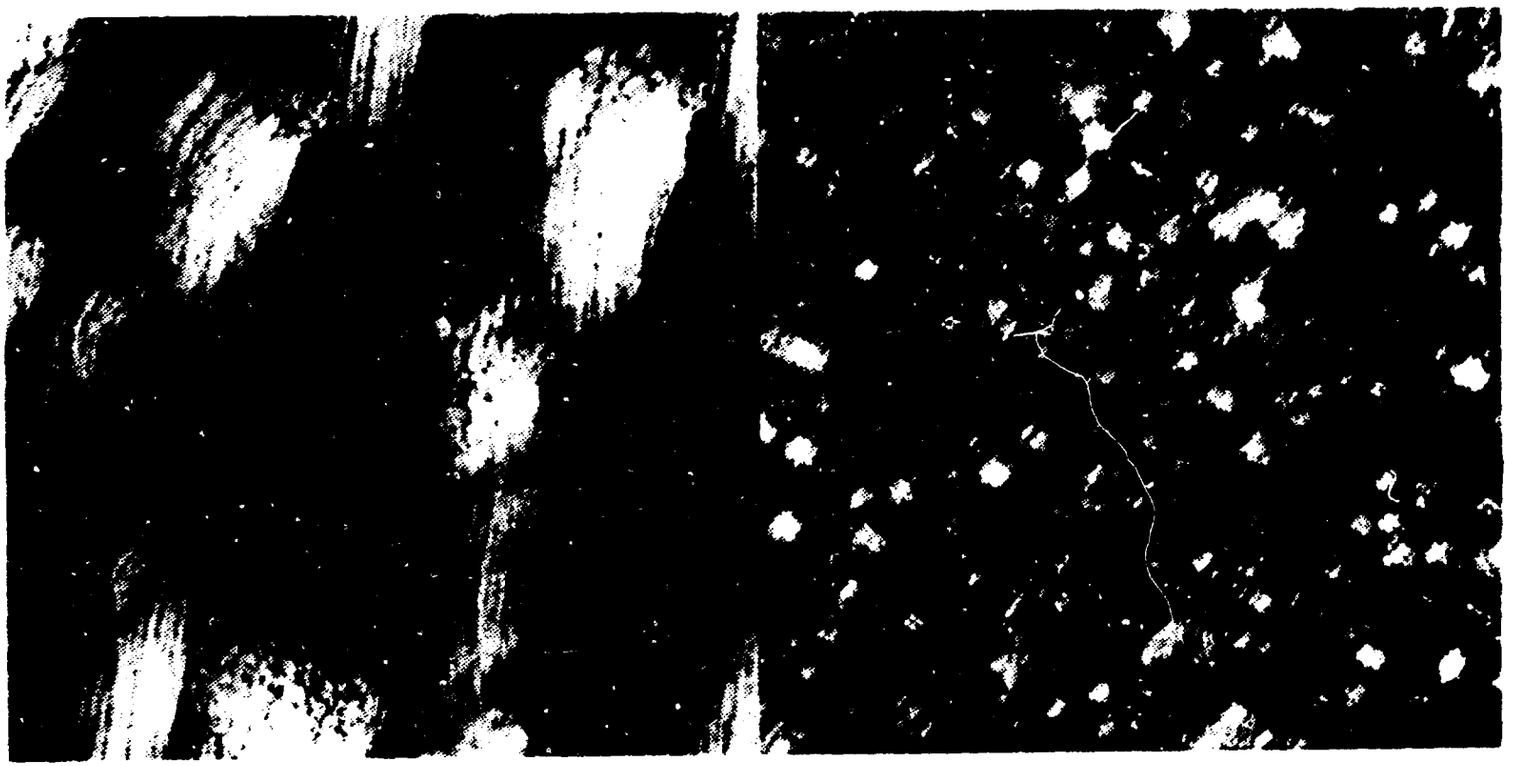

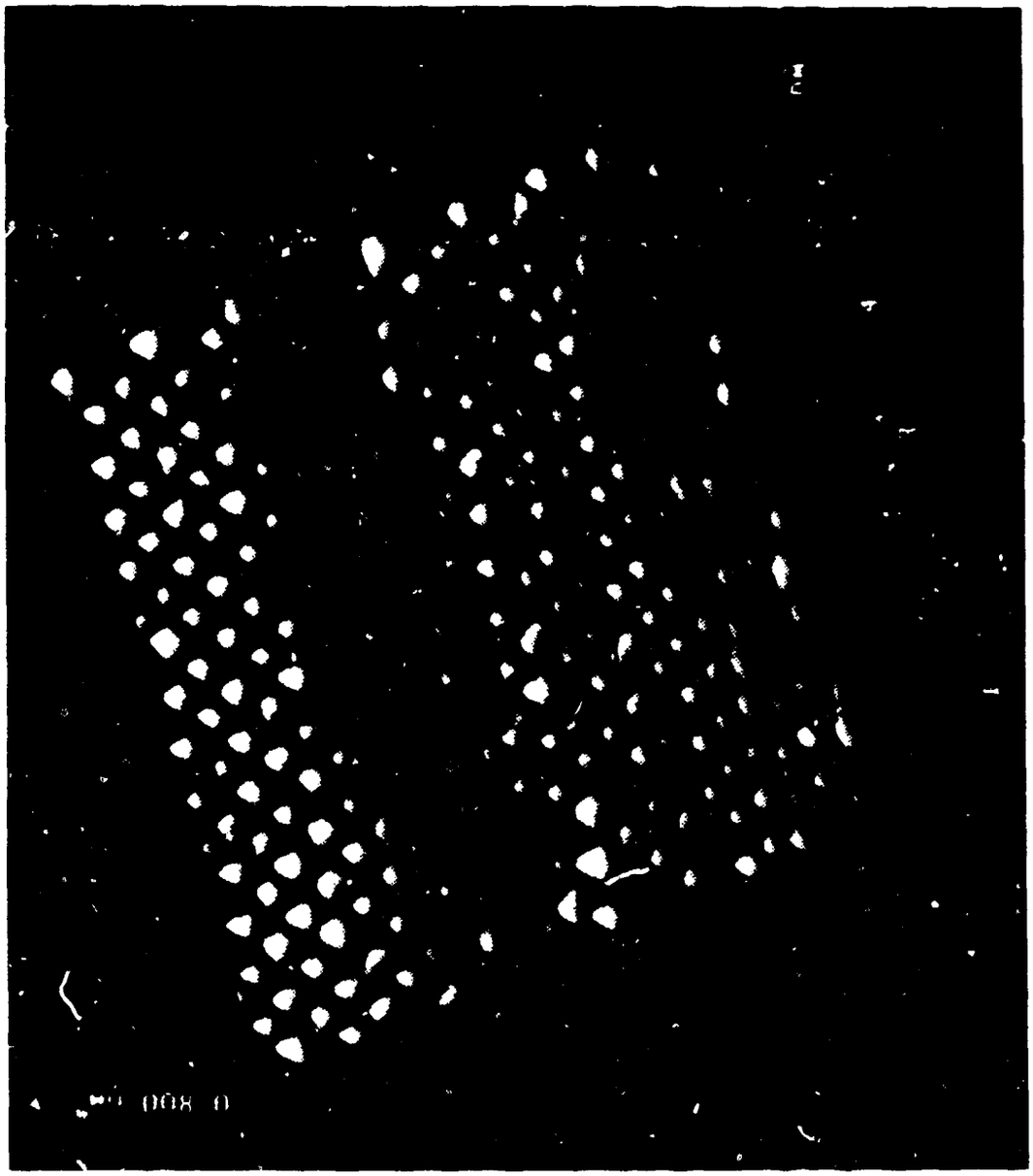

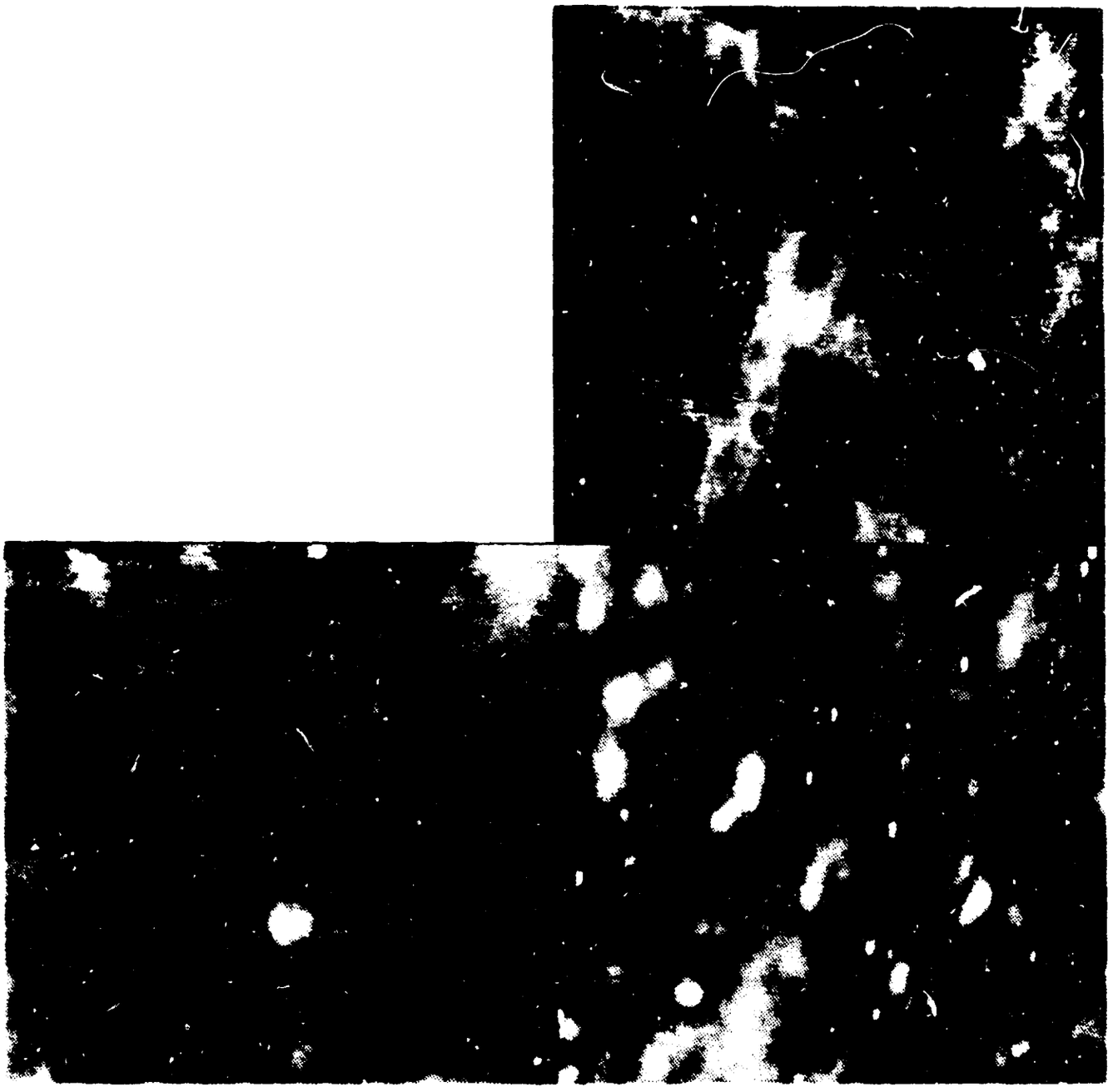

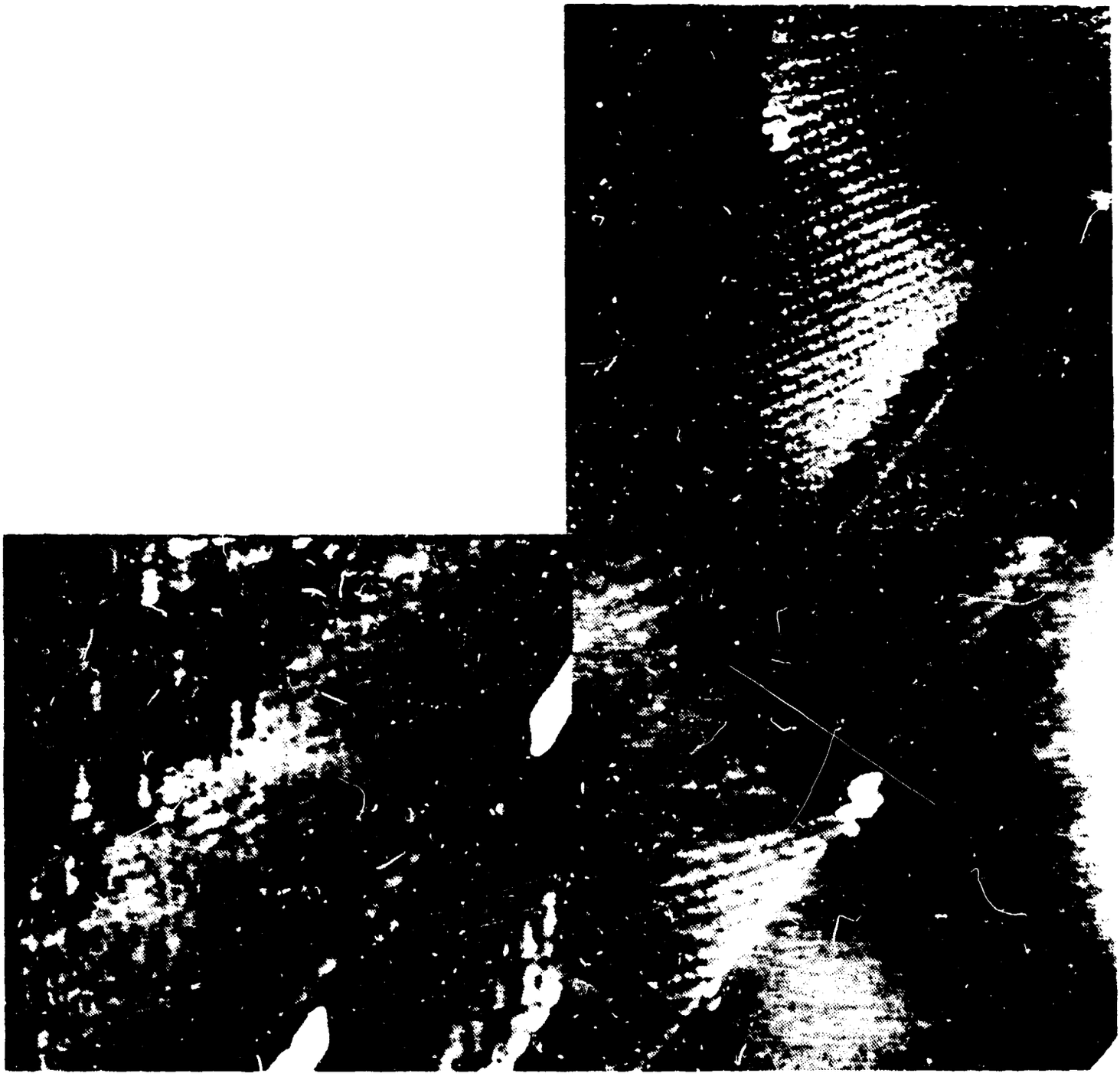

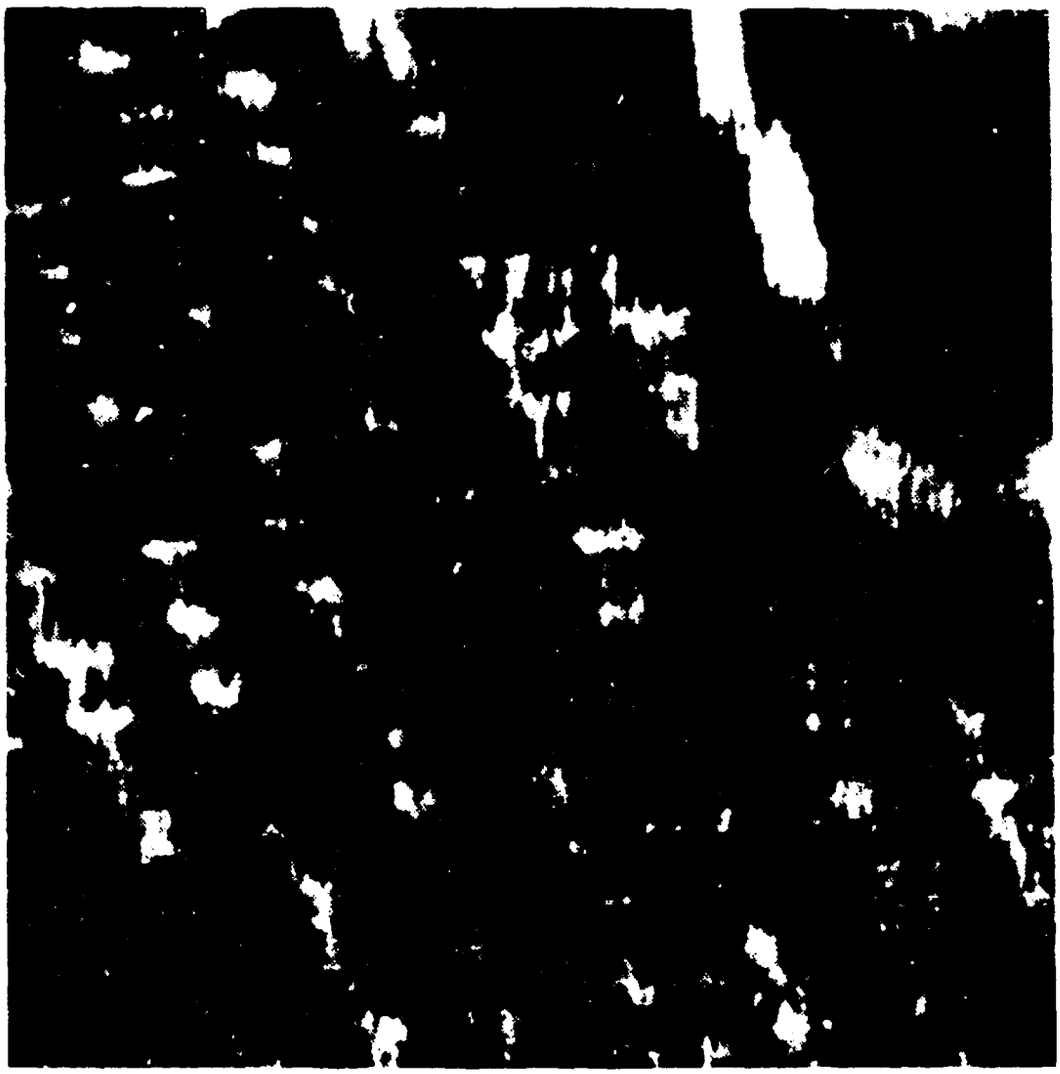

Height Angle Clear Calc

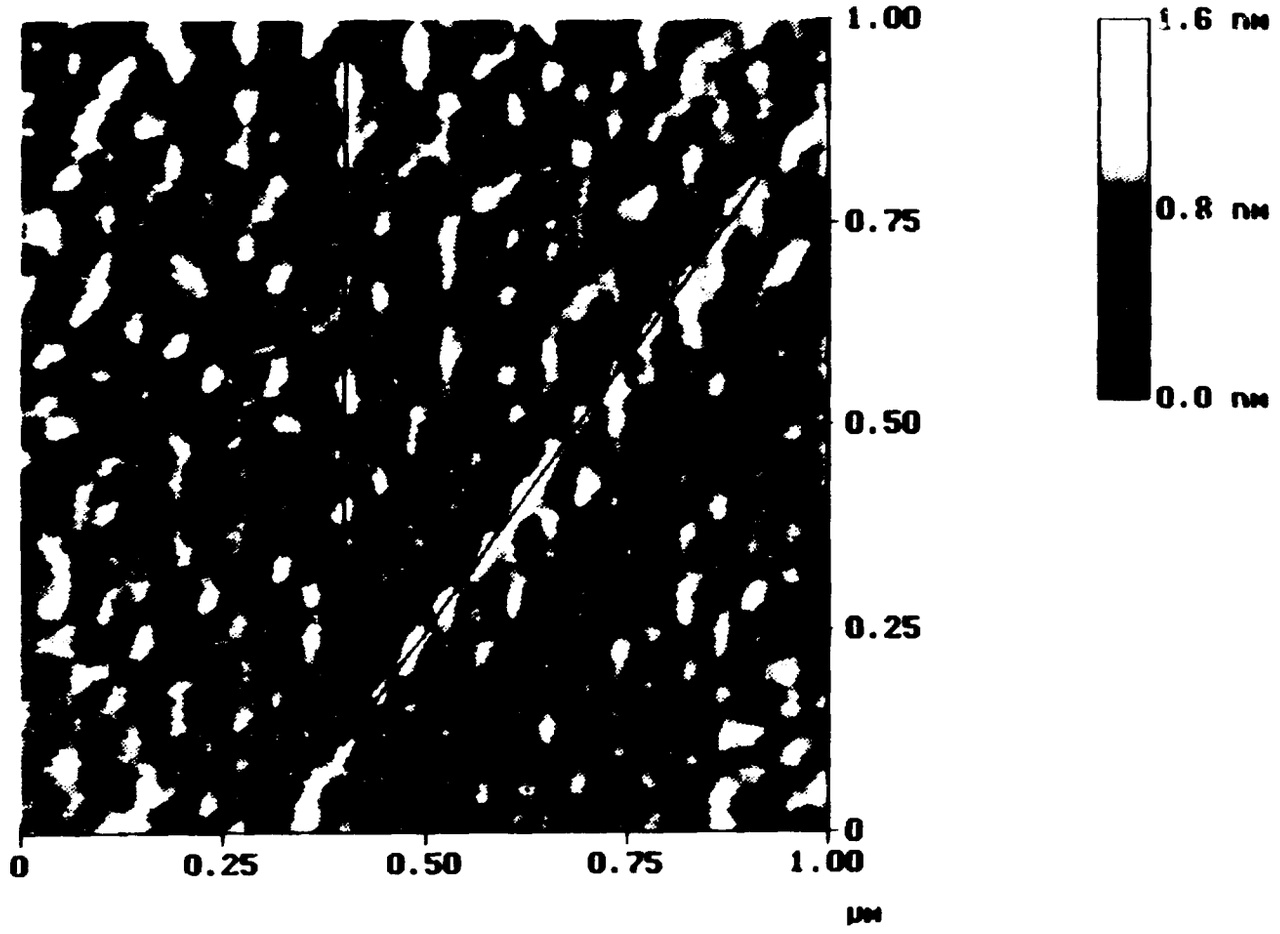

GOET9-2.131 BLADES GOETHITE DRIED RMS=1.6A

Angle 36.41 degrees